THE EMISSION/ABSORPTION FE II SPECTRUM OF HD 45677

R. Stalio and P.L. Selvelli
Astronomical Observatory of Trieste
Italy

ABSTRACT

The complex behavior of the Emission/Absorption spectrum of Fe II is analyzed. The far UV spectrum is characterized almost solely by absorption lines, while, in the near UV, strong emissions are predominant. Radiative excitation from the ground to the highest levels ($\chi \simeq 10$ eV) with re-emission in the near UV, visible and I.R. seems to be the main mechanism capable of explaining the observed spectral features.

THE EMISSION/ABSORPTION SCHEME

The emission-line star HD 45677 (a short summary of its main observed characteristics is presented in Table 1) shows a Fe II spectrum which appears as (1) sharp in absorption with typical Be-shell-phase profiles; (2) sharp in emission in its forbidden components, (3) wider in emission, sometimes with sharp absorption on the blue wing. This variety of profiles is present throughout the different spectral ranges observed: the passage from shell-phase-like profiles to emission is gradual as one moves from the ultraviolet below 2000 Å to longer wavelengths. There is probably a "null" region, around 2100 Å, where absorptions and emissions are balanced. Above 2300 Å the lines are in emission, but the strongest ones show a reversal on the blue wing. In the visual this characteristic is enhanced, the emission appearing as split into two components. All forbidden Fe II lines are in the visual-near IR ranges. The usually expected inter/circumstellar Fe II absorptions are observed between 2300 and 2600 Å superimposed on the corresponding stellar emissions.

The only important exception to the above scheme is due to multiplet UV 191, in emission at about 1786 Å. Figure 1 illustrates some of the behaviors described above.

Ni shows the same behavior, the passage from absorptions to emissions being observed in a more restricted wavelength range from 1200 to 1750 Å. Other emission lines in the ultraviolet spectrum are OI at λ1305 and the Mg II resonance doublets. At λ1641.2 there is also an unidentified strong emission that was incorrectly attributed to He II: it cannot be He II because the wavelength displacement is too large and its presence would be in contradiction with the generally low ionization character of the emission spectrum.

II. THE GROTRIAN DIAGRAM

We restrict the analysis to that portion of the energy level diagram formed by the term systems of the quadruplets and of the sextets. The extension to the doublets follows naturally. Octets are unimportant. One must recall that deviations from LS coupling can be important for Fe II, so that intercombination transitions must be taken into account.

If we consider only the sextets, we see from Figure 2 that transitions between the ground term a^6D and the closest ones a^6S (multiplet 7F), $z^6D°$ (multiplet UV1), $z^6F°$ (UV2), $z^6P°$ (UV3) correspond to actually observed emission lines. On the contrary, as the excitation potential of the upper terms increases, we observe the transitions a^6D-$y^6P°$ and a^6D-$x^6P°$ in absorption. The terms $y^6P°$ and $x^6P°$ emit to the metastable term a^6S (multiplet UV 191), which in turn emits to the a^6D. Trnasitions from the ground to higher energy terms, as for example a^6D-$w^6P°$ (EP high=11.30 eV, multiplet UV18) fall below the wavelength range of IUE. As the correlated downward transition to a^6S is not observed either in emission or in absorption, we guess that there is not enough flux reaching the region of formation of Fe II lines to cause excitation above about 10 eV. Partial support for this idea comes from a comparison of the transition probabilities and the observed line strengths. The oscillator strengths for the transitions a^6S-$x^6P°$ and a^6S-$w^6P°$ are comparable; conversely only the lines of the lower energy transition (multiplet 191) are seen in emission. Thus the situation can be represented by a simple three-level-atom scheme, the levels being the terms a^6D, a^6S and either $y^6P°$ or $x^6P°$: we observe high frequency quanta being transformed into low frequency quanta through radiative processes occurring in diluted radiation fields. The high energy quanta are radiated in the Balmer continuum of the B2 stellar photosphere. Part of these quanta have energy sufficient to excite Fe II until about 10 eV; not more, because the flux of a B2 star falls down steeply shortward of Ly α.

A similar three-level-atom scheme holds for the quadruplets and doublets. A partial energy transition scheme for the quadruplets is given in Figure 2b. All the levels of the lowest even terms are excited to high energy levels ($\Delta E \geq 7$eV) of the permitted odd terms. These last emit to the metastable levels around 3 eV, which in turn emit to the lowest even terms via forbidden transitions observed in the visual-near IR range.

NI shows the same behavior for the $2p^3\ ^2D°$, $2p^3\ ^2P°$ and $3S^2P$ terms, the lower term $2p^3\ ^2P°$ being excited to $3S^2P$, 8.3 eV above.

The three-level-atom scheme, however, explains only partially the observed emissions. It is not very evident what is the source of excitation of the odd-term-z-levels. In Figure 2a we see, for example, that two strong emissions (the multiplets UV3 and V42) depart from $z^6P°$, despite the fact that there is no evident way of feeding it. The emissions corresponding to the transition $z^6P°-e^6D$ are, in fact, too weak; intercombination transitions do not seem to play any role in this case. Also for the quadruplets and doublets the z levels behave in this way. We have not yet, carefully checked the influence of intercombinations in these cases.

III. CONCLUSIONS

It is still too early to draw definite conclusions from our observations. HD 45677 is not a very common object, although the features that we have briefly described in Table 1 and called "stellar" are characteristic of all early-type stars: the profiles of the "sensitive" lines give evidence of motions, and there is mild superionization (NV seems to be absent) indicating chromospheric-coronal regions.

The unusualness lies in the cool "metallic" line spectrum, essentially Fe II. The concomitant presence of absorption lines in the far-UV, permitted emissions in the near UV and permitted-forbidden emissions in the visible and near-IR suggests a simple explanation in terms of resonance fluorescence from the ground terms under conditions of diluted radiation and matter density.

However, the difficulty of explaining a number of emission line strengths, as for example that of multiplets UV3 and V42, makes us reluctant to assume the resonance fluorescence mechanism as the only possible one: there might be other mechanisms, like pumping from other ions, which produce part of the observed emission spectrum.

In our case it is possible that a clue towards a better understanding of the odd-term-z-level excitation will come from IUE observations with a high signal-over-noise ratio in that region that we have called "null", around 2100 Å.

TABLE 1

m_V = 8.5-9.5	Presently fading in light
Spectral type: B2	From visual and UV spectral energy distribution. IR excess.
E (B-V): 0.15	From the "bump" at λ2175.
IUE high resolution observations:	2xLWR: the emission strength has declined from the first (Sept 1978) to the second observation (March 1979); 1xSWP (March 1979).
IUE "stellar" absorption spectrum:	C IV and Si IV are the highest ionization states definitely present; undisplaced resonance lines observed; FWHM 250 and 40 km s^{-1} respectively. Al III resonance doublet and Fe III (multiplet 34) with abrupt rising of the blue wing to the continuum.
IUE emission spectrum:	described in the text.

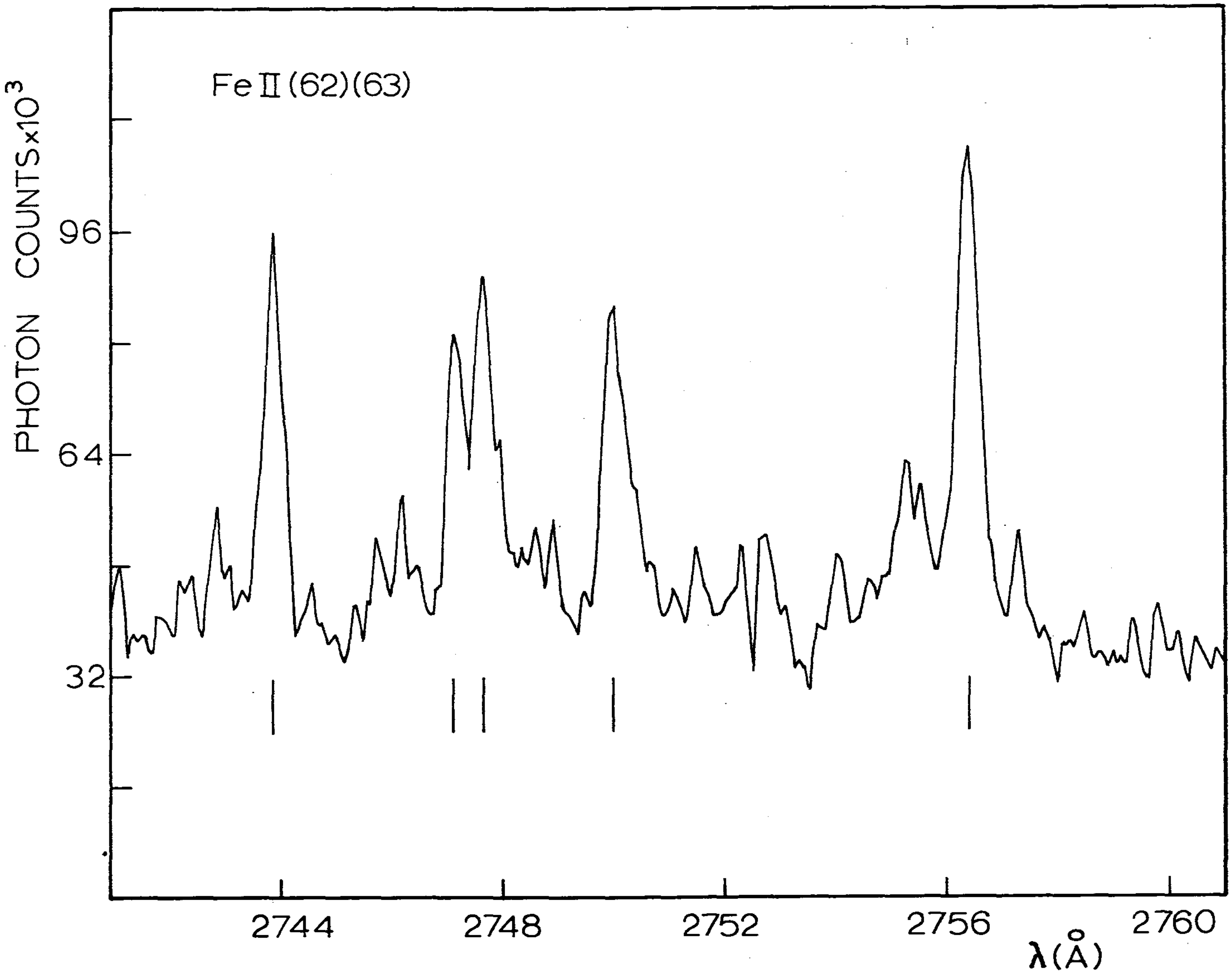
Fe II (62)(63)
PHOTON COUNTS×10^3
96
64
32
2744
2748
2752
2756
2760
λ(Å)

Figure 1

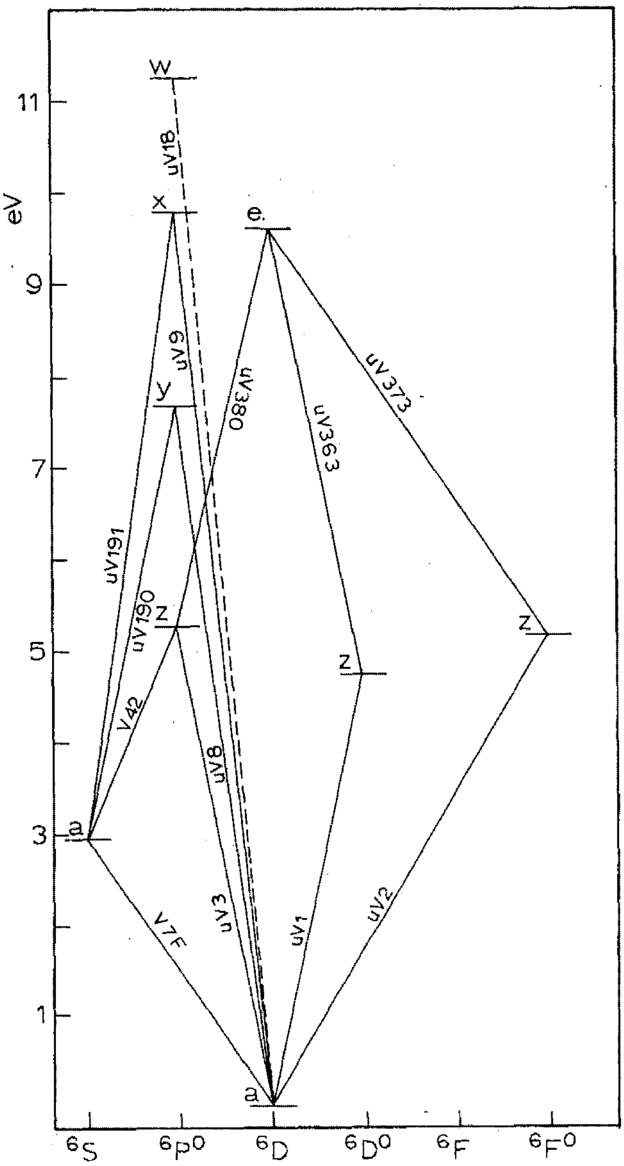

eV
11
9
7
5
3
1
w
x
e
y
z
z
z
a
a
uV18
uV9
uV380
uV373
uV363
uV191
uV190
V42
uV8
uV3
V7F
uV1
uV2
^6S
$^6P^0$
^6D
$^6D^0$
^6F
$^6F^0$

Figure 2a

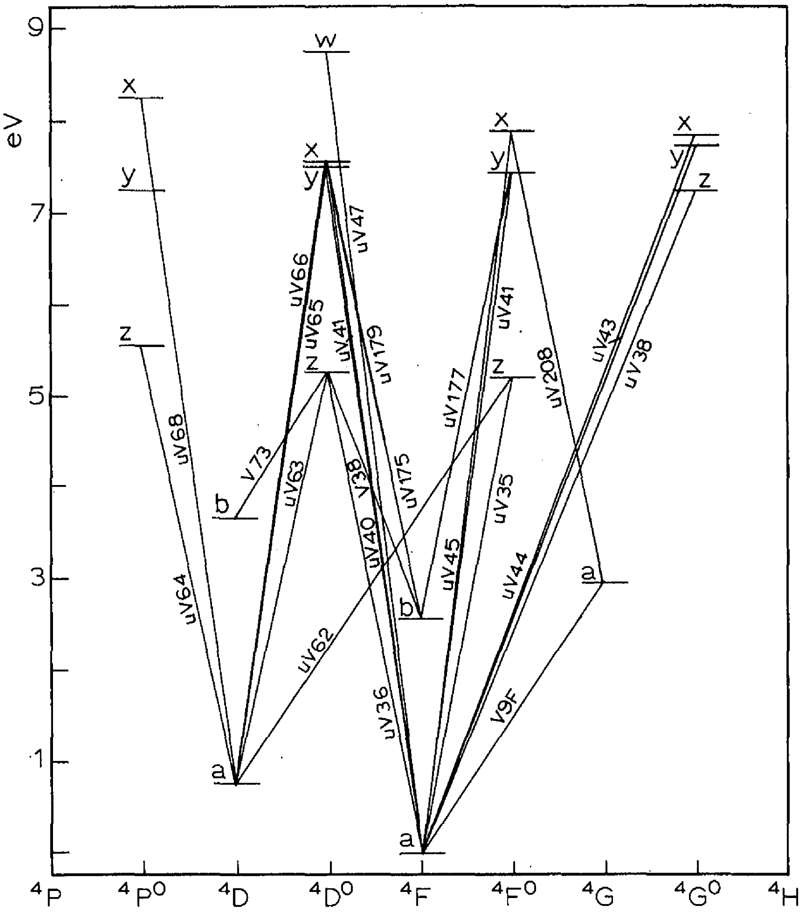

eV
9
7
5
3
1
x
y
z
b
a
w
x
y
z
b
a
x
y
z
a
x
y
z
uV68
uV64
V73
uV63
uV66
uV65
uV41
uV62
V38
uV40
uV36
uV47
uV179
uV175
uV177
uV45
uV41
uV35
uV208
uV44
uV43
uV38
V9F
4P
4P0
4D
4D0
4F
4F0
4G
4G0
4H

Figure 2b